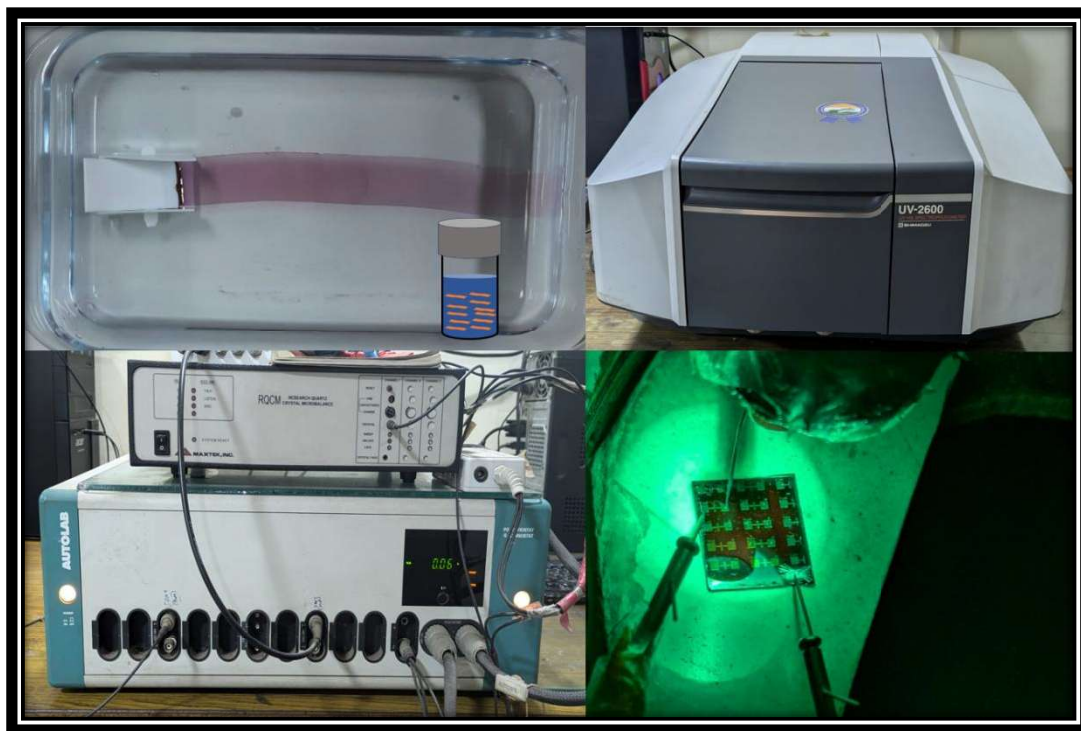


## Chapter 2

### *Experimental and Instrumentations*



*This chapter delves to the theoretical underpinnings of experimental methods that were used to characterize the materials that were synthesized. For structural, morphological, and electrical analyses, a variety of advanced instruments are used to examine the polymers and their nanocomposites. To give a thorough grasp of each technique's function in describing material qualities, it is described together with the equipment that goes along with it.*



## **2.1.Introduction**

In this chapter, experimental techniques have been discussed that are used to fabricate and assess high-performance organic thin films and devices. One key strategy of my PhD work was to optimize the selection of material along with appropriate processing techniques so as to meet the primary goal of developing low-cost fabrication techniques that reduce defects. Therefore, materials include high-purity organic semiconductors, dielectrics, and various substrates that are selected in compatibility with the processing techniques to meet the stringent requirements of electronic performance. Besides, different deposition methods like; spin coating, floating film transfer method (FTM), unidirectional floating film transfer method (UFTM), and thermal evaporation are used to fabricate thin film devices. A stiff control was exercised over the concentration of the solutions, spin speed, as well as substrate temperature in order to obtain homogeneous and defect-free films. Finally, a number of advanced characterization techniques were employed to completely grasp the structural, morphological, as well as electronic properties of the prepared films. AFM was applied in the research investigation of surface morphology and nanoscale irregularities within the films. Beyond that, the crystallinity and molecular alignment in the films were explored with the help of XRD and polarized UV-Visible spectroscopy. Details crystallographic orientation and phase purity of the thin films were obtained from thin-film X-ray diffraction, and polarized UV-Visible spectroscopy. These studies help to determine the film anisotropy, which are very important studies to optimize charge transport in devices. The morphology of the samples was characterized using high resolution scanning electron microscopy (HR-SEM). Besides, time resolved second harmonic generation was used to analyze the non-linear optical properties of the films, which elucidates the dynamic processes associated with the films. Electrochemical behavior of the films has been studied by cyclic voltammetry (CV) experiments to verify the HOMO level of the polymer thin

films. Finally, the chapter ends with the fabrication and measurement of OFETs and OPTs devices. Evaluation under controlled conditions offer deep insight into the correlations between the structure and properties and factors responsible for better charge transport occurring within the films. Electrochemical behavior of films was studied by CV to confirm the HOMO level of the polymer thin films. Finally, the electrical characterization of OFETs and OPTs devices were performed using semiconductor parameter analyser.

### 2.2. Materials:

Among the semiconductors used, DPP-TTT (with two different molecular weights) and P4T2F-HD were purchased from Ossila, and their chemical structure is shown in *Figure 2.1 (a) and 2.1 (b)* respectively. While  $C_3N_5$  was synthesized in the lab using 3-amino-1,2,4-triazole (3AT) and its chemical structure is shown in *Figure 2.1 (c)*. Additionally, octadecyltrichlorosilane (ODTS) was purchased from Sigma Aldrich. The polytetrafluoroethylene (PTFE) syringe filters and Hellmanex solution were also sourced from Ossila UK. Other chemicals, including dehydrated chloroform, glycerol, ethylene glycol, acetone, isopropanol alcohol (IPA), and methanol, were procured from TCI Chemicals, Japan, and SRL, India. All commercially sourced chemicals were used without further purification unless otherwise specified.

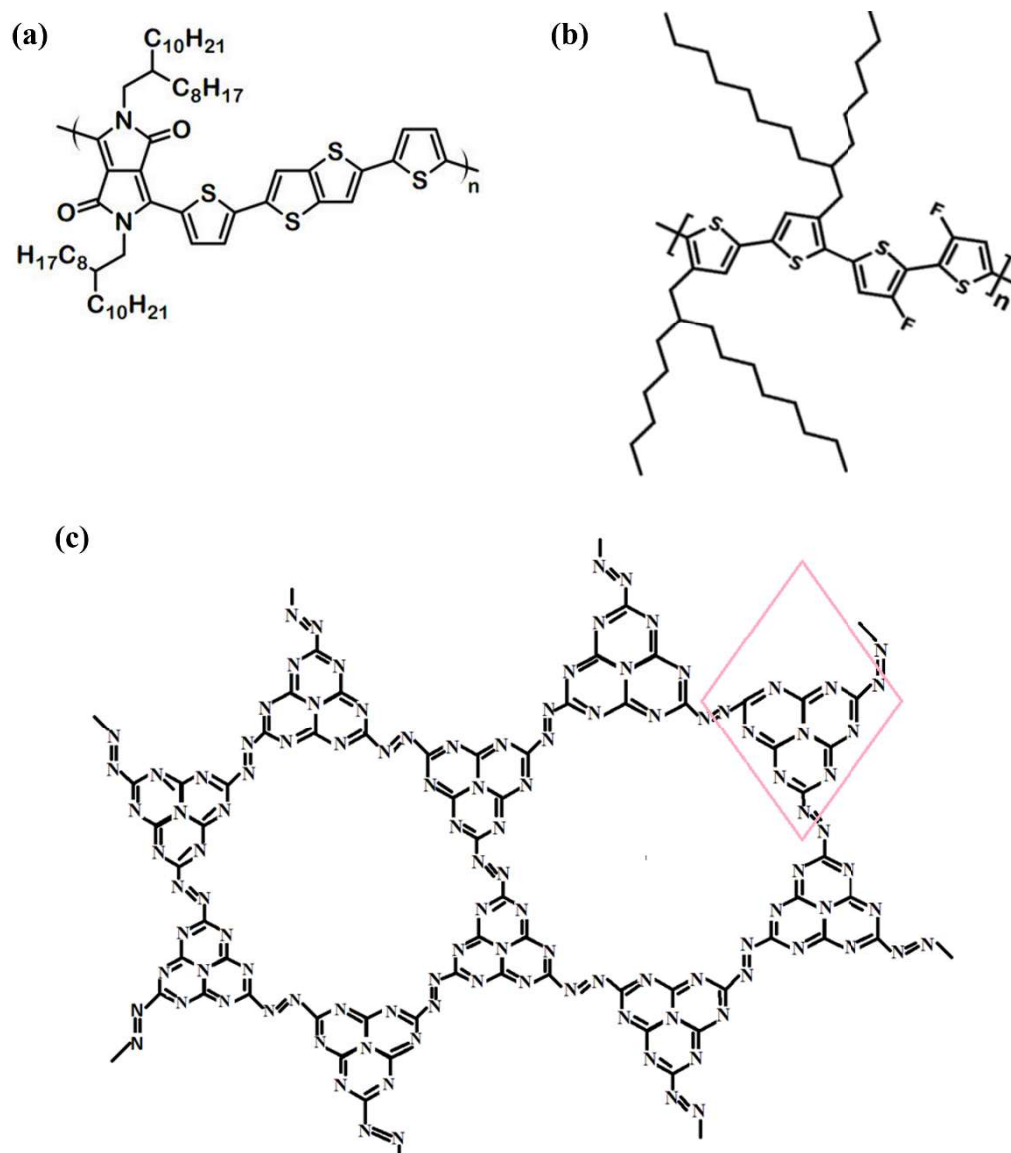


**Figure 2.1** Chemical structure of (a) DPP-TTT (b) P4T2F-HD, (c) C<sub>3</sub>N<sub>5</sub>.

## 2.3. Materials Synthesis

### 2.3.1. Synthesis of C<sub>3</sub>N<sub>5</sub>:

The synthesis of C<sub>3</sub>N<sub>5</sub> began with the carbonization of (3AT) at 500 °C, using a heating rate of 3 °C/min over a 3 h duration in a muffle furnace under ambient air conditions, as depicted in **Figure 2.2**. After this thermal treatment, an orange tint became apparent in naturally cooled C<sub>3</sub>N<sub>5</sub>[62, 63]. The as-synthesized C<sub>3</sub>N<sub>5</sub> material then underwent

mechanical crushing using a mortar and pestle, which was utilized for subsequent characterizations.

To exfoliate  $C_3N_5$  into few-layered nanosheets, a 5 mg sample of bulk  $C_3N_5$  was dispersed in 2 mL of water and then subjected to vigorous probe sonication for a period of 3 h, ensuring comprehensive dispersion and transformation of the bulk material into nanosheets. After the sonication step, the resultant material was carefully centrifuged to separate the larger  $C_3N_5$  particles from exfoliated few-layered  $C_3N_5$ . The separated bulk components were then dried and weighed to determine the yield of nanosheets. To ensure that only the portion rich in nanosheets is used, the homogeneous supernatant solution, free from larger particles and impurities, was extracted and utilized as the initial material for subsequent experimental procedures.

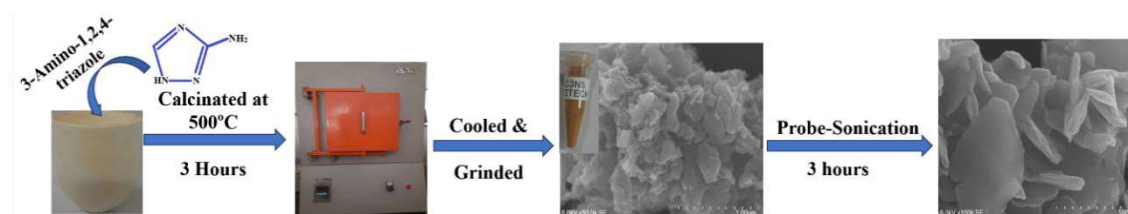


**Figure 2. 2** Schematic representation of  $C_3N_5$  synthesis from its precursor.

### 2.3.2. Dielectric Synthesis:

#### 2.3.2.1. Li- $Al_2O_3$ Ion-Conducting Gate Dielectric Solution Synthesis:

The Lithium Alumina ( $Li-Al_2O_3$ ) dielectric solution was synthesized by a solution-based method. Initially, two separate solutions of lithium acetate and aluminum nitrate with concentration of 500 mM were prepared using Lithium acetate ( $LiOOCCH_3$ ) (>99.5% purity, Sigma Aldrich) and Aluminium nitrate nonahydrate ( $Al(NO_3)_3 \cdot 9H_2O$ ) (>98% purity, Sigma Aldrich) precursors, by dissolving in 2-methoxy ethanol. These solutions were stirred vigorously for 1 hour at room temperature. Subsequently, the lithium nitrate and aluminum nitrate solutions were mixed in 1:11 to form a 500 mM lithium alumina

precursor solution[64]. This mixture underwent continuous stirring for 6 hours. Prior to spin coating, the Li-Al<sub>2</sub>O<sub>3</sub> solution was filtered using a 0.45 μm PVDF syringe filter to eliminate larger particles.

### **2.3.2.2. Poly (methyl methacrylate) (PMMA) Dielectric Preparation:**

The molecular weight (Mw) of poly (methyl methacrylate) (PMMA) that were used as gate dielectric of organic transistors, was ~50,000 g/mol. PMMA was dissolved in toluene to a concentration of 40 mg/mL at 700 rpm through constant magnetic stirring for 12 hours for complete dissolution[65]. The solution was ultrasonicated for 20 minutes to remove any remaining undissolved polymer aggregates. The obtained PMMA solution was filtered by using a 0.45 μm PVDF filter to remove the residue particulates for homogeneity of the solution. Then the filtered PMMA solution was spun coated on the flexible ITO-coated PET substrate using a spin-coating process at 2000 rpm speed for 60 seconds. After spin coating, the substrate coated with PMMA was annealed at 100°C for 30 minutes for better adhesion and uniformity of the film, thus enhancing the quality of the coating in general.

### **2.3.3. Polymer Ink Preparation:**

#### **2.3.3.1. Preparation of Polymer Solution:**

Preparation of a solution at 15 mg/mL using chloroform as the solvent. The polymer was dissolved in chloroform, which was then heated at 60°C for 30 minutes to get complete dissolution [66]. Any undissolved residues were removed. Further sonication for 10 minutes was done and used for thin film preparation.

#### **2.3.3.2. Preparation of Polymer/C<sub>3</sub>N<sub>5</sub> Solution:**

The DPP-TTT/C<sub>3</sub>N<sub>5</sub> nanohybrid preparation entailed drying the water dispersion of C<sub>3</sub>N<sub>5</sub> nanosheets to prepare a homogeneous chloroform dispersion. Then, the solution of the C<sub>3</sub>N<sub>5</sub> nanosheet with a series of required quantities (1%, 3%, and 5% of the concentration

of polymer) was slowly added into the 10 mg/ml DPP-TTT chloroform solution. After that, the solution was stirred at a controlled temperature of 50 °C for 12 hours[52]. This resulted in the gradual evaporation of the solvent and thus concentrated solution. To ensure the chloroform properly mixed with all the solutions resulting in appropriate concentration levels, the same was added uniformly to all the solutions. The compound was then left sealed for a prolonged period of 48 hours, ensuring adequate stirring and fully integrated hybrid material.

### **2.4. Thin Film Fabrication Techniques:**

#### **2.4.1. Spin Coating:**

Spin coating is one of the most commonly used techniques for the fabrication of thin films from organic semiconductor solutions. This technique is known for being simple, and capable of producing uniform layers. A small amount of organic semiconductor solution is first deposited onto the center of a substrate. The substrate subsequently undergoes rapid rotation at very high speeds; usually, speeds between 500 and 5000 RPM. The action of spinning generates centrifugal force, due to which the solution spreads uniformly over the surface. Next, a thin film is created by evaporation of the solvent in the solution while the substrate keeps spinning. The thickness and quality of the resulting film depend on several parameters such as the rotational speed, the viscosity of the solution, and the rate of solvent evaporation; its instrument and steps are shown in *Figure 2.3 (a) and 2.3 (b)* respectively. Higher spin speeds normally result in thinner films, though the viscosity of the solution was pivotal in the uniformity of the film. The film morphology is also affected by evaporation of the solvent; fast evaporation can be the precursor to defects such as pinholes, whereas slower evaporation tends towards smoother and more uniform films. It is highly advantageous for organic semiconductor films due to their production of very uniform layers that are basic to the efficiency of semiconductor devices.

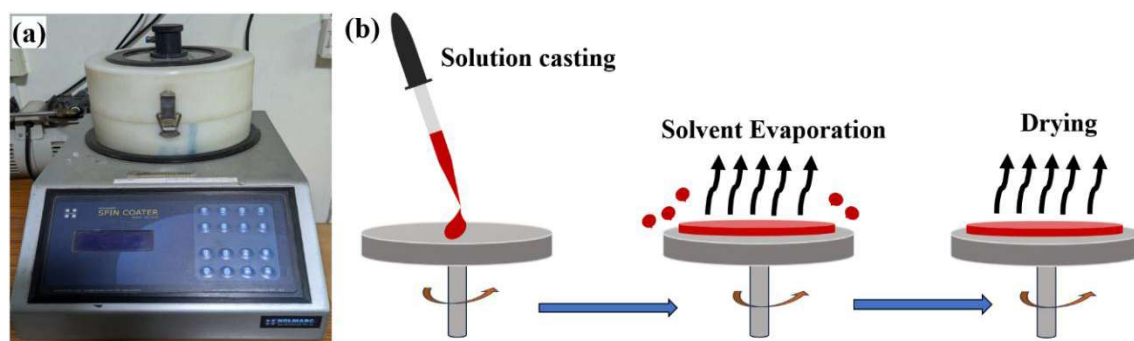


**Figure 2.3** (a) Photographs of Spin coating instruments (b) schematic representation of the steps involved in spin coating process.

#### 2.4.2. Floating Film Transfer Method:

For thin film deposition through the FTM method, I prepared a mixture of Ethylene Glycol and Glycerol in a 1:1 ratio. This mixture was thoroughly blended using magnetic stirring for 30 minutes at 40°C. After achieving a homogeneous solution, it was poured into a Petri dish. Next, 10-15  $\mu\text{l}$  of the polymer ink with low surface energy was carefully placed in the center of the Petri dish, at the air-liquid interface of the high surface energy liquid mixture as shown in **Figure 2.4**. As the polymer solution is deposited onto the liquid substrate, it begins to spread across the surface while the solvent simultaneously evaporates. The spreading of the polymer solution is primarily influenced by the surface tension forces at play. The spreading coefficient,  $S = \sigma_1 - \sigma_s - \sigma_{1s}$ , determines whether the polymeric solution will spread or contract. Here,  $\sigma_1$  is the surface tension of the liquid subphase,  $\sigma_s$  is the surface tension of the polymer solution, and  $\sigma_{1s}$  is the interfacial tension between the liquid and the polymer solution. A positive value of  $S$  indicates that the surface tension gradient at the liquid-liquid interface is favorable, causing the polymeric ink to spread spontaneously outward. Simultaneously, the viscous, hydrophobic nature of the liquid substrate exerts a force opposing the expansion of the polymer film. This counteracting force, combined with the rapid evaporation of the solvent, causes the polymer backbones to align, resulting in an oriented thin film. The quality and morphology of this film can be fine-tuned by adjusting

various casting parameters, including the concentration of the polymer solution, the viscosity of the liquid substrate, and the temperature at which the substrate is maintained. These factors collectively influence the balance of forces and the dynamics of the spreading process, ultimately determining the characteristics of the final thin film.

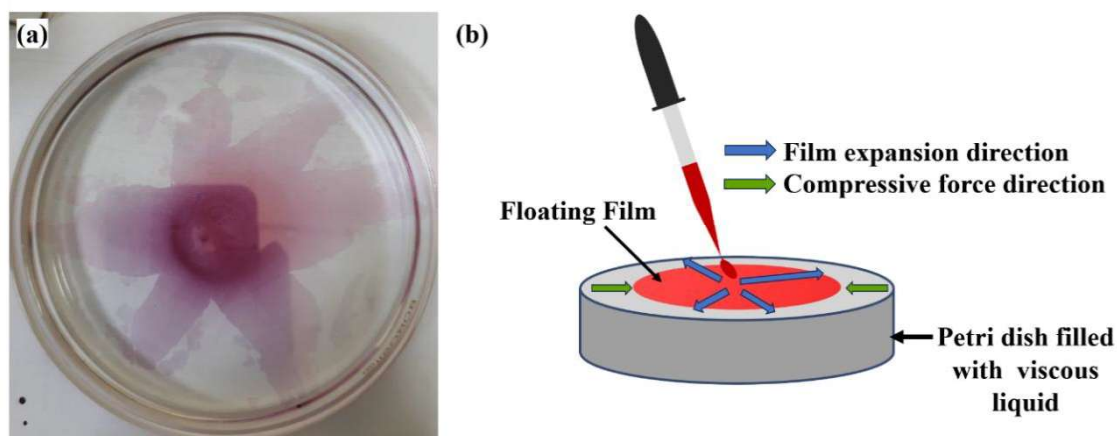


**Figure 2. 4** (a) Photographs of the FTM thin film (b) schematic representation of FTM and their steps involved during film fabrication.

### 2.4.3. Unidirectional Floating Film Transfer Method:

The UFTM is a method of application to obtain a precisely controlled unidirectional orientation of polymer chains. In this respect, the UFTM allows for the control over the orientation of OFET chains, which is the key point in optimizing the OFET's performance, as seen in **Figure 2.5**. A polymer solution is cast on the top of a phase-separated liquid and then dries up to form a thin film. The film is then transferred onto a solid substrate. Since the controlled, unidirectional motion of the slider aligns polymer chains parallel to the direction of transfer, the technique leaves behind a uniform, highly oriented layer of polymer, which is critical for the ability to enhance both structural and electronic properties in the resulting OFET devices.

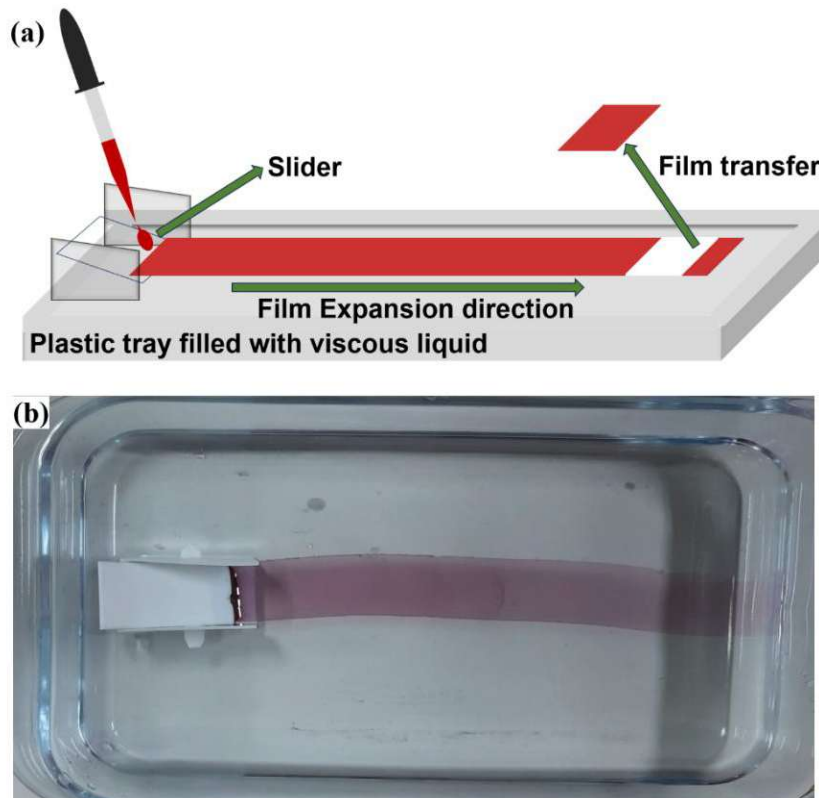


**Figure 2.5** (a) Schematic representation of the UFTM (b) photographs of the UFTM thin film.

#### 2.4.4. Polydimethylsiloxanes (PDMS) Mold:

This is one of the techniques which is based on mold and lithography combined as explained Polydimethylsiloxanes (PDMS) Mold fabrication involves a simple soft lithography technique extensively used in pattern replication at the micro- and nanoscale as shown in **Figure 2.6**. A master is first formed by using conventional photolithography on a silicon wafer to define the features of interest. PDMS prepolymer is then formed by mixing base and curing agent in the weight ratio 10:1, followed by degassing to remove air bubbles[67]. The PDMS is poured onto the master mold and degassed again prior to curing in an oven at 60–80 °C for 1–2 hours. The PDMS is then peeled off the mold after curing, creating a negative copy of the master pattern. For certain applications, such as microfluidic device fabrication, the surface of the PDMS can be

treated with oxygen plasma to enable permanent bonding with glass or a second layer of PDMS.

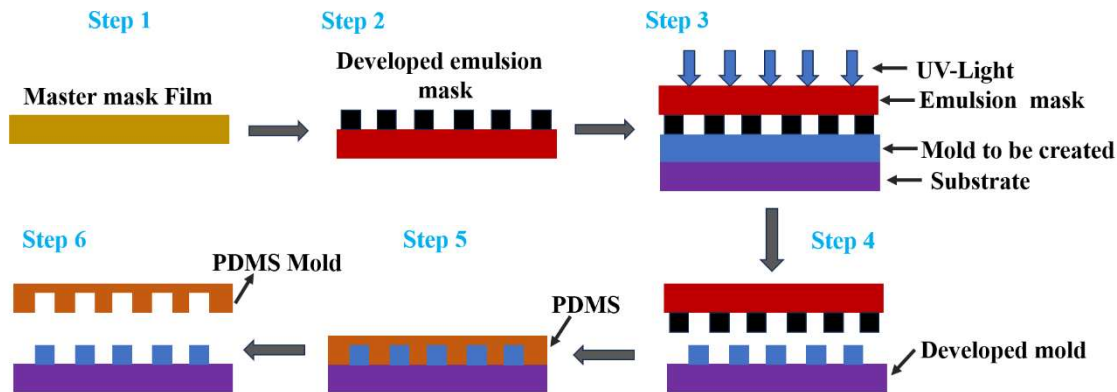


**Figure 2. 6.** Schematic Representation of PDMS mold preparation.

## 2.5. Device Fabrication:

### 2.5.1. Substrate Preparation:

Heavily p-doped silicon (p<sup>+</sup>-Si), ITO coated PET, and SiO<sub>2</sub> dielectric layer on highly n-doped Si substrates were used for different thin film device fabrication. Before device fabrication, substrates were cleaned to ensure the removal of any organic or inorganic impurities that could affect device performance. The cleaning process began with an initial treatment using a Hellmanex solution, followed by rinsing in deionized (DI) water to remove surface contaminants. Subsequently, the substrates were cleaned sequentially in acetone, DI water, and IPA for 15 minutes each, using ultrasonication to ensure the effective removal of residues. After these wet cleaning, the substrates were subjected to a plasma cleaning process as shown in **Figure 2.7**, followed by thermal annealing at 120 °C for 30 minutes. Further modification on the SiO<sub>2</sub> and other dielectric coated substrate surface was carried out by the treatment of the ODTs. For that treatment, first of all, a 10 mM solution of ODTs was prepared in toluene. Substrates were then immersed in that solution and allowed to react for 1 hour at room temperature. This process allows a self-

assembled monolayer to form on the surface, which changes the properties of the surface; typically, it is rendered more hydrophobic. The substrates were then removed carefully from the ODTS solution after treatment for 1 hour and rinsed thoroughly with fresh toluene to washout unbound ODTS molecules. The substrates were then dried under a stream of nitrogen gas to ensure that the surface treated is clean and ready for further processing.

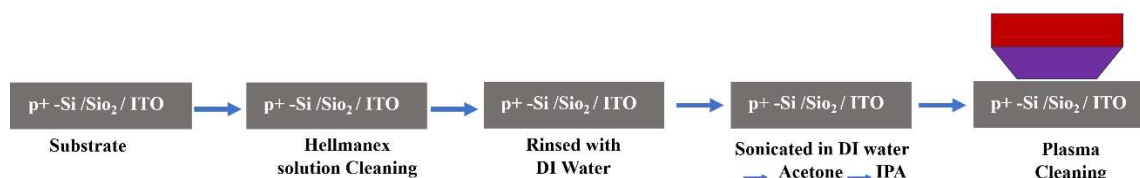


**Figure 2. 7** Schematic representation for the substrate cleaning.

### 2.5.2. Metal-Insulator-Metal Device Fabrication:

A step-by-step approach ensured the dielectric thin film was characterized by fabrication of the Metal-Insulator-Metal device. The process began with a preparation of a heavily p-doped silicon substrate which was of 15 mm × 15 mm. It was properly cleaned following the standard RCA cleaning procedure to remove organic, ionic, or any particulate contaminants as shown in **Figure 2.7**. On the cleaned substrate, a dielectric layer of Li-Al<sub>2</sub>O<sub>3</sub> was deposited. This was done with the use of the precursor solution spun at 5000 rpm for 50 seconds onto the cleaned substrate. From the spin coating process, there was a uniform distribution of the precursor solution across the substrate surface. After coating, the substrate was dried on the preheated hot plate at 70°C for 2 minutes to remove any residual solvents. Annealing in a furnace for 30 min at 350°C helped to convert the precursor salts into a uniform metal oxide thin film. The above process of coating and annealing was cycled three times to obtain a desired film thickness. Lastly, the Li-Al<sub>2</sub>O<sub>3</sub> thin film was partially crystallized by the final annealing step that took place at 500°C for an hour. In the case of PMMA dielectric thin film fabrication, a PMMA solution of

concentration 40 mg/ml was spun onto the  $n^+$ -Si/SiO<sub>2</sub> substrate at 2000 rpm for 1 minute and then annealed at 100°C for 30 minutes. The fabrication process is completed by depositing a 70 nm thick aluminum (Al) electrode directly onto the dielectric layer through a sputtering process, as depicted in **Figure 2.8**. This electrode served as the top contact for the MIM structure, thereby completing the device and rendering it ready for dielectric characterization studies.

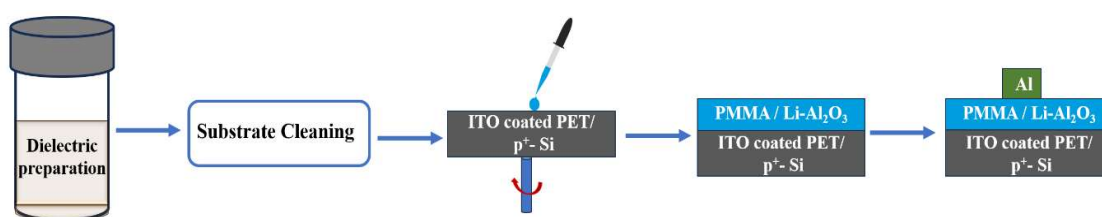


**Figure 2. 8** Schematic representation of the MIM ( $p^+$ -Si/dielectric/Al) device fabrication.

### 2.5.3. Active Layer Fabrication for OFETs:

For organic semiconductors, isotropic thin films are often produced via spin-coating to achieve uniformity across all directions. To create oriented thin films with directional molecular alignment, techniques such as FTM, and UFTM were used, allowing for enhanced control over film orientation and properties.

### 2.5.4. Electrode Deposition using Thermal Vapour Evaporator:

The top electrode of the OFETs such as source and drain were fabricated through thermal vapour deposition (TVD) (Hind High Vacuum instruments) using nickel shadow mask as per the desired channel length and width shown in **Figure 2.9**.

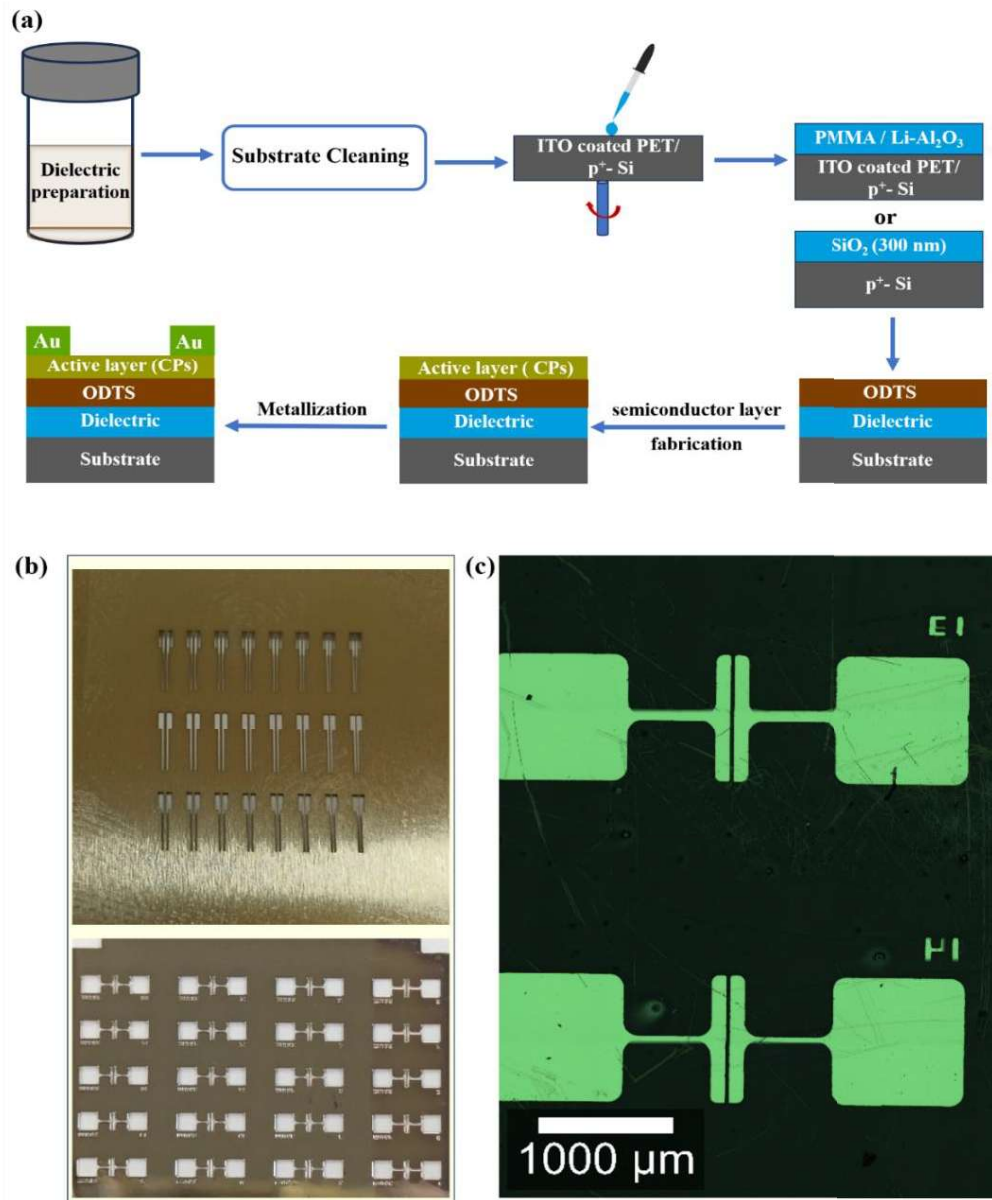


**Figure 2. 9** (a) Representation of the OFETs fabrication (b) photographs of the nickel shadow mask (c) optical images of the shadow mask.

TVD operates on the principle of vaporizing a solid material in a high-vacuum environment and allowing the vaporized atoms or molecules to condense on a substrate, forming a thin film. The system consists of several critical components, each essential for achieving precise and high-quality deposition. The vacuum chamber maintains a high vacuum, typically in the range of  $10^{-5}$  to  $10^{-7}$  Torr, which minimizes contamination and ensures that the vaporized material travels with minimal interaction with residual gas molecules. This

is essential in achieving a high-purity film. The source of heat is what causes the material to vaporize. This can be through a resistive heater, that heats the material via electrical resistance, or an electron beam, which focuses high-energy electrons onto the material to vaporize it. The evaporation source, or boat, holds the material and is made of materials resistant to high temperatures and impurities' introduction. The substrate holder positions the substrate above the evaporation source. This can then be heated or rotated to ensure uniform deposition of the film and improve adhesion of the film on the substrate. The atoms or molecules vaporized condense into an ultrathin film, uniform over the substrate which was measured by a quartz crystal thickness monitor.

## **2.6. Characterizations Tools:**

### **2.6.1. Structural Characterizations:**

**2.6.1.1. X-ray Diffraction (XRD):** XRD is a great analytical technique that determines the crystallographic structure, phase composition, and other structural properties of a material. The principle of XRD is founded on the principle of constructive interference between monochromatic X-rays scattered by periodic atomic planes existing in the crystalline material. When a beam of X-rays is directed toward any sample of any crystalline substance, the X-rays scatter the atoms in the crystal lattice. The scattered X-rays overlap constructively at certain angles, known as Bragg angles, to produce a diffraction pattern characteristic of the material's crystalline structure. The main parts of an XRD system are the x-ray source generally being a sealed tube or rotating anode, producing the X-rays through bombarding with high-energy electrons a target material that is most typically made of copper. The resulting X-rays filtered to produce a monochromatic beam are directed towards the sample. The goniometer is a precision instrument where the sample and detector can be accurately adjusted in terms of their relative angles to measure the

diffraction angle. The sample holder is used to orient the crystalline sample along the direction of the X-ray beam. Proper alignment of the sample is very critical because it provides conditions such that the incident X-ray will interact with the crystalline planes at the right angles. The detector records the diffracted X-rays at different angles, so as to measure the intensity. A schematic for Bragg diffraction and X-Ray diffractometer is provided in *Figure 2.10*.

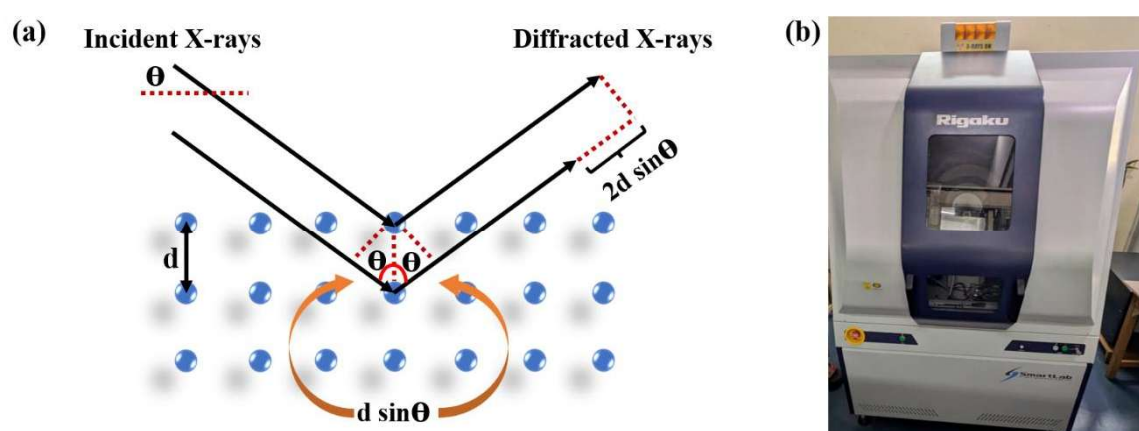


**Figure 2.10** (a) Schematic representation of XRD<sup>[68]</sup> (b) instrument image of the thin film XRD

#### 2.6.1.2. Fourier Transform Infrared Spectroscopy (FTIR):

FTIR is an extremely versatile and one of the most widely used techniques for analytical purposes, concerning identification, characterization of materials by showing the absorption of infrared (IR) radiation. The basic principle for FTIR is that IR radiation passes through a sample in which some wavelengths are specifically absorbed by the molecules of the sample leading to vibration according to the frequencies unique to the chemical bonds present in the material. Those vibrations are pertinent only to the energy differences between vibrational states of molecules, and therefore they give rise to a characteristic "molecular fingerprint," which can be stored as an IR spectrum. The FTIR instrument is

comprised of several key components that work in harmony to give this spectrum. An infrared source sends out IR radiation over a wide spectrum, often from a glower of silicon carbide or a Nernst glower, which radiates IR in the continuous spectrum when heated. The main part of the FTIR is the interferometer, which consists of a beam splitter, a fixed mirror, and a moving mirror. The beam splitter splits the incoming IR beam, which allows it to take two paths—the first to the fixed mirror and the second to the moving mirror. The two beams are reflected back to and recombine at the beam splitter to form an interference pattern, called an interferogram, that holds all the spectral information contained in the sample. The sample is placed in a sample holder where it interacts with the IR radiation. Depending on the vibrational modes of the molecules present, as well as whether the radiation goes through or bounces off the sample, certain wavelengths get absorbed. The detector measures the intensity of the transmitted or reflected IR radiation; this signal gets converted to electrical form. The IR spectrum resulting provides in-depth information regarding the molecular composition and the structure of the sample, thus enabling it to identify functional groups as well as analyze interactions at the molecular level. The basic principle is depicted in *Figure 2.11* along with the instrument.

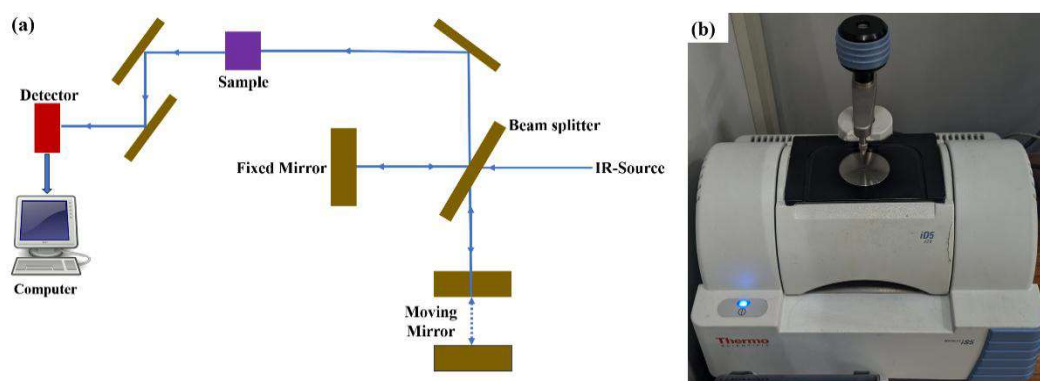


**Figure 2. 11** (a) Schematic representation of the FTIR (b) photographs of the FTIR instrument.

### 2.6.1.3. X-ray Photoelectron Spectroscopy (XPS):

X-ray photoelectron spectroscopy is a surface-sensitive analytical technique that can characterize the elemental composition, chemical state, and electronic state of elements within the top few nanometers of the material's surface. XPS is based on the principle of the photoelectric effect where X-rays induce emission of core electrons from the surface of a material. The kinetic energy of these emitted electrons is measured; with this, the binding energy of the electrons can then be determined, shown in *Figure 2.12*. Since the different elements and chemical states have unique binding energies, elements present on the surface are identified and quantified. It contains an X-ray source, such as aluminum (Al  $K\alpha$ ) or magnesium (Mg  $K\alpha$ ), that is used to generate the X-rays which ionize the core electrons. This is then measured by the electron analyzer in terms of the kinetic energy of the outgoing electrons, while the detector records electron counts. This spectrum is a plot of the number of electrons versus their binding energy, giving information about the elemental composition and chemical environment of atoms on the surface.

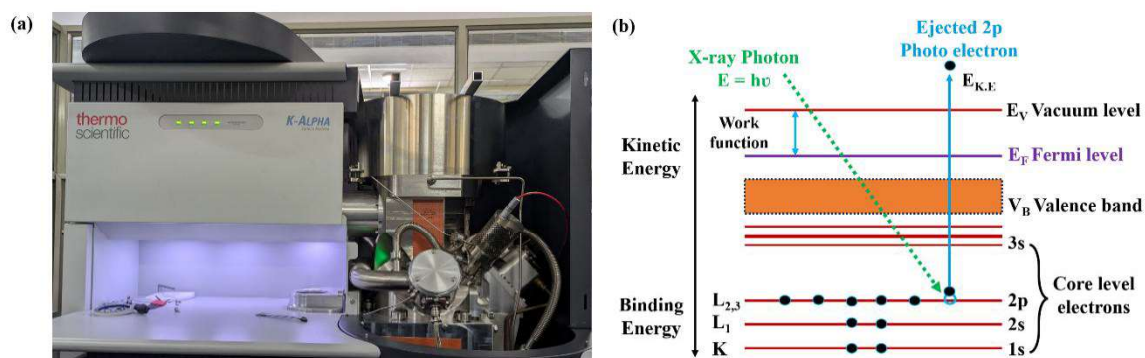


**Figure 2. 12** (a) Represents the Photographs of the XPS instrument (curtsy to CIFC IIT BHU), (b) working principle of the XPS

---

---

**2.6.2. Optical Characterizations:****2.6.2.1. UV-Visible Spectroscopy:**

UV-Visible spectroscopy is an important tool for the investigation of the optical properties of organic materials, especially those featuring  $\pi$ -electron systems. In such systems, incident light can excite  $\pi$  electrons from their ground state  $\pi$  to an excited  $\pi^*$  state. This is best done at some wavelength dependent on the energy gap between the two, called  $\lambda_{\max}$ . This is influenced by the crystallinity of the thin film and thus allows one to gain insight into the material itself in greater detail. In this work, UV-Visible-NIR absorption spectroscopy was applied in the study of a polymer thin film coated on a quartz substrate. The analysis was carried out using a dual-beam spectrophotometer Shimadzu 2600. The optical anisotropy within the thin film was studied further by introducing a Glan–Thompson prism between the sample and the light source. This anisotropy of the thin film arises due to the alignment of the polymer backbones within the film. Whenever linearly polarized light is incident on the film, the absorption varies with the orientation of the polarization relative to the polymer backbone. The absorption is maximum if the polarization is parallel to the backbone direction, while minimum absorption is observed when the polarization is perpendicular to it. This difference in absorption allows for the definition of a dichroic ratio DR defined as  $DR = A_{\parallel}/A_{\perp}$ . Thus, by definition,  $A_{\parallel}$  is the maximum absorbance at  $\lambda_{\max}$  when incident light is polarized parallel to the backbone and the meaning of  $A_{\perp}$  is the absorbance when light polarization is perpendicular. The dichroic ratio attaches a number value to the level of orientation in the thin film relative to its optical anisotropy. The setup of UV-Vis spectrophotometer is given in *Figure 2.13*

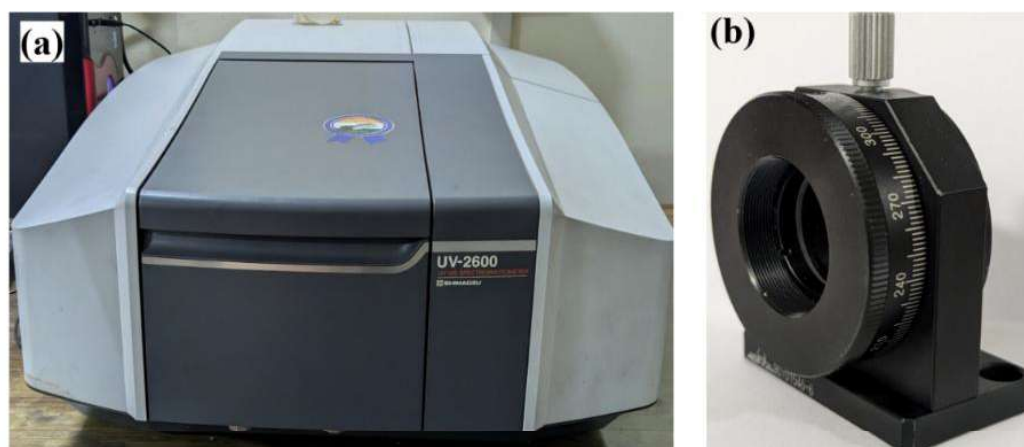


*Figure 2.13 (a) Photographs of The UV instrument (b) photograph of the polarizer.*

### **2.6.3. Surface and Morphological Characterizations:**

#### **2.6.3.1. Atomic Force Microscopy (AFM):**

AFM is highly sensitive to the imaging and measuring of surface properties of materials at a nanoscale resolution, providing detailed insights into surface topography, mechanical properties, among others. The working principle of the AFM principle is associated with the forced interaction between a very sharp tip attached at a flexible cantilever and the surface under investigation. While scanning along the surface, the tip experiences quite a number of forces: van der Waals forces, electrostatic forces, and even some mechanical contact forces that make the cantilever bend. A laser beam focused onto the back of the cantilever tracks these deflections by bouncing back off the cantilever onto a photodetector. Surface scans are rendered into an image of the surface topography at atomic or molecular resolution in recognition of those interactions at the tip with the surface by using the photodetector to measure the minute deflection from the cantilever. The mechanism is shown in *Figure 2.14*. The AFM system is made up of several critical components: the cantilever with a sharp tip, interacting with the surface of the sample; laser monitoring the deflection of the cantilever; photodetector detecting the reflected signal of laser; and a

piezoelectric scanner carefully controlling in three dimensions the displacement of sample or the tip. AFM can operate in various modes, such as contact mode, where the tip is constantly in contact with the surface; tapping mode, where the tip intermittently touches the surface; and non-contact mode, where the tip is above the surface and is not in direct contact with it. These various modes make AFM capable of rendering accurate information about the surface morphology and the material properties under different conditions.

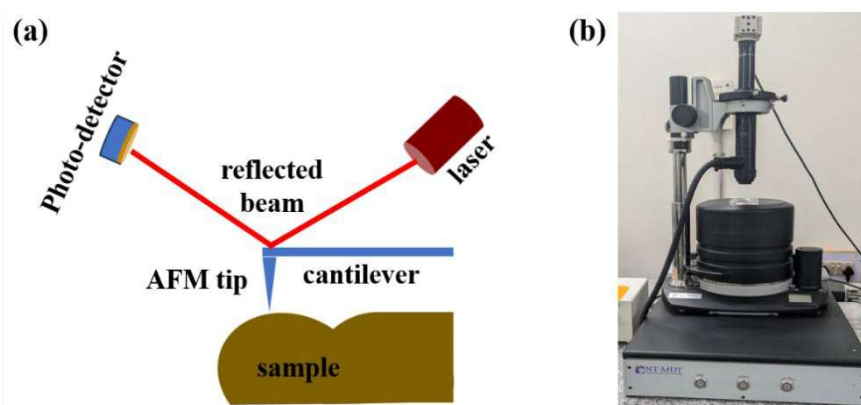


**Figure 2. 14** (a) Schematic representation of the AFM (b) photographs of the AFM instruments.

### 2.6.3.2. Scanning Electron Microscopy (SEM):

SEM is a high-resolution instrument used to image surface morphology at the nanoscale. Thin imaging process required a beam of high-energy electrons that bombard onto the specimen surface. At the point of interaction, these electrons with the atoms in the sample produce several signals, including secondary electrons (SE), backscattered electrons (BSE), and characteristic X-rays, each carrying different information. The core part of SEM is the electron gun, which may be regarded as a source of the electron beam. The emitted electrons are focused into a fine beam by a series of electromagnetic lenses. The condenser lens controls the diameter of the beam and the objective lens focuses it precisely onto the

sample's surface. Scanning coils then systematically deflect the beam in a raster pattern across the sample, allowing the SEM to build an image by collecting data from each point the beam touches. The secondary electrons produced through this interaction are low-energy electrons emitted from the surface of the sample, and thus a SEM can provide images of the surface topography at quite high resolutions where the fine structural details of the sample are revealed. Backscattered electrons (BSE), high energy electrons, that reflect from the sample offer contrast depending on the differences in atomic numbers making them excellent for compositional analysis. Characteristic X-rays are also generated by the interaction of the electron beam with the sample and can be detected using detectors to provide elemental composition information apt for fine chemical analysis. Vacuum system consists of several pumps which continuously remove the air and other gases from the chamber. It ensures a high-vacuum operation of the SEM. Such vacuuming is essential to maintain the needed focus and intensity of the electron beam with an objective of producing high-quality images and getting accurate data. A basic schematic for SEM is provided in *Figure 2.15*.

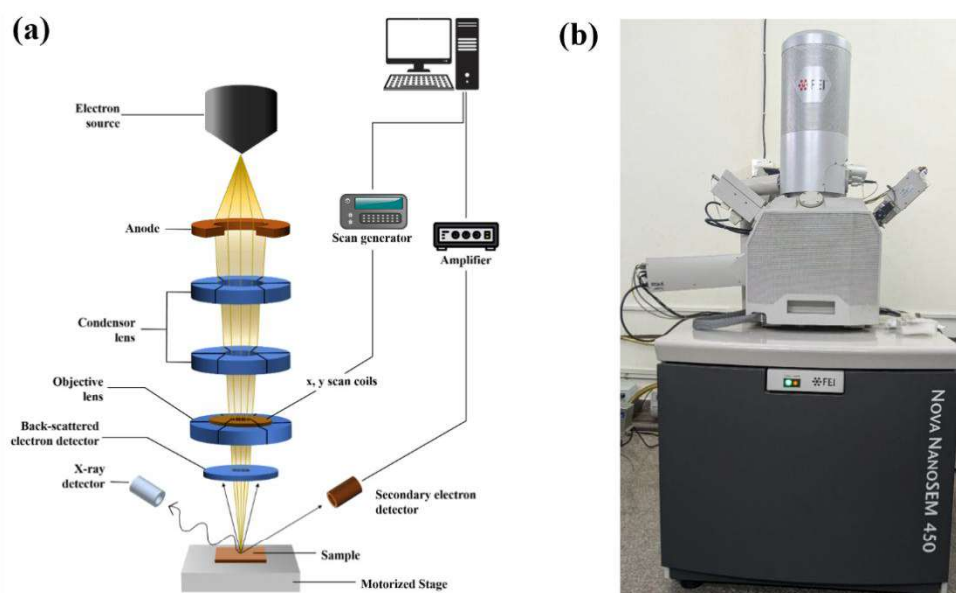


**Figure 2. 15 (a) Schematic representation of the SEM (b) instrument image**

## 2.6.4. Electrochemical Characterizations:

### 2.6.4.1. Cyclic Voltammetry:

CV is an electrochemical potentiodynamic technique that has been highly exploited for establishing redox activity of electroactive species and insight into a complex chemical reaction resultant from electron transfer processes, including catalysis. In a typical CV experiment, the potential applied on the working electrode is swept between two set potential limits in opposite directions and the resulting current is measured. This is achieved through a three-electrode system that possesses an electrode, labelled as the working electrode, and where the redox reaction occurs, and another, termed the counter, which balances the current flowing in and out. The other type is the reference electrode used for measuring the potential difference. All the electrodes are immersed in an electrolyte solution. The counter electrode completes the electrical circuit, whereas the reference electrode with a known standard potential measure the working electrode's potential, providing a stable point of reference. Recorded data appear in the form of a cyclic voltammogram, current plotted against the applied potential, which can provide ample

information regarding the electrochemical properties of the system under study. The schematic of the instrument is provided in *Figure 2.16*. Once the CV ramp reaches the set upper or lower limit, it is reversed; this can be repeated multiple times in one experiment. It is this cycle that causes redox peaks to occur and provides information about the electronic structure and behavior of the analyte.

To study the influence of various internal microstructures on the position of the (HOMO) in organic semiconductor thin films, the CV measurement was performed in a non-aqueous electrolyte of 0.1 M solution of TBAP in ACN. The working electrode was prepared by transferring the UFTM film onto an ITO substrate of a geometric area  $1\text{ cm} \times 1\text{ cm}$ . Reference was the standard Ag/AgCl electrode, and the counter electrode was prepared in the form of coiled platinum wire. The CV scans were recorded after purging the electrolyte solution with high-purity nitrogen gas to remove the dissolved oxygen that could affect the measurement. The working electrode was dipped into the electrolyte solution to ensure proper diffusion before the start of the experiment. All CV scans were recorded in the dark. Some cycles of CV were performed at the initial stages so that the system could stabilize and provide consistent data. The HOMO position was achieved from a reference to the redox potential of the standard compound, such as ferrocene. It was then correlated into energy levels using established equations.

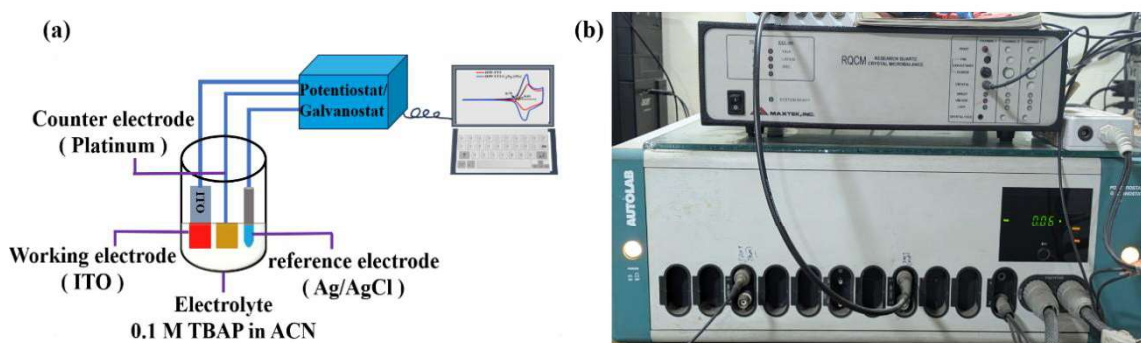


**Figure 2.16** (a) Schematic representation of the CV instrument (b) instruments photographs of cyclic voltammetry.

## 2.6.5. Electrical Characterization:

### 2.6.5.1. Capacitance vs. Frequency Measurement:

In order to evaluate the quality of the dielectric thin film as a gate dielectric for OFETs, I carried out current versus frequency (I-f) measurements. This measurement was made using a MIM device structure to mimic the scenario that would prevail in the operation of the dielectric layer in a transistor. The capacitor effective area in the MIM structure was defined by the mask used at the metallization step of the top electrode, thus enabling precise control over the measurement parameters. Current response of the dielectric layer to varying frequencies was measured with a  $p^+$ -Si/dielectric/Al device using an LCR meter from Keysight (Keysight LCR meter E4990A). The measurements were performed across a frequency 100 Hz to 10 MHz, with applied AC voltage of 50 mV. These C-f characterizations are very important to determine the dielectric properties, dielectric constants, and nature of frequency-dependent behavior in the dielectric material involved in OFETs. The structures employed for these measurements are presented in **Figure 2.8**, which are the same as those used in capacitance-frequency analysis.

---

---

**2.6.5.2. Leakage Current Measurement:**

The assessment of leakage current density is considered as the important step of assessing quality before using it in dielectric thin films for creating TFTs. In an ideal case, the sandwiching by a dielectric thin film between two electrodes of metal should not allow any kind of current passage. However, in practical uses, imperfections as fine as traces or pinholes in the thin film can be critical enough to allow a small amount of current to leak through. This measurement is very important to predict the behavior of leakage current when the same dielectric thin film is used for the fabrication of TFTs. Characterizing this, the current-density-voltage (J-V) characteristics were measured of MIM devices configured as  $p^+$ -Si/dielectric/Al. The measurements were all performed in an open atmosphere with the help of an Agilent B1500A semiconductor parameter analyser.

**2.6.5.3. Thin Film Transistor Characterization:**

Since OFETs are three terminal devices two primary measurements are needed to express the electrical characteristics. First measurements are output characteristics in which the drain current,  $I_D$  is plotted against the drain voltage,  $V_D$  at a constant gate voltage,  $V_G$ . This  $V_D$  vs.  $I_D$  characterization defines the linear and saturation regions of the OFET, ensuring the correct operation of the device. The second set of I-V measurements is called transfer characteristics, which involves measuring  $I_D$  as a function of varying  $V_G$  under a constant  $V_D$  ( $I_D$  vs.  $V_G$ ). The transfer characteristics of OFET are very crucial because they define essentially the key parameters such as field-effect mobility, the ratio of on/off currents, and the threshold voltage,  $V_{th}$ . Electrical characterizations were conducted under light illumination of different intensities by using a semiconductor parameter analyzer Agilent B1500A along with a source meter from Keithley, 2612. OFET electrical contacts were shaped with the assistance of a probe micromanipulator to achieve measurements to

be of a high accuracy. Electron mobility for the device has been determined from the transfer characteristics using the gradual channel approximation method.

**2.6.5.4. Current vs Time ( $I-t$ ) Characterization:**

The transient photoresponse of the transistor was characterized with measurements of conducting current versus time. This two-probe technique represents a suitable tool for measuring the transient response of the device, depending on the level of illumination. Such information about the response time of the transistor to light stimuli can be gained by tracking the change in current over time. Such information allows insight into whether the device is efficient and fast as a phototransistor. With this approach, one could accurately estimate how fast the transistor would respond to changes in light intensity. This makes it ideal for applications requiring rapid responses to photoexcitation.

**2.6.5.5. Time Resolved Microscopic Second Harmonic Generation Technique:**

To explain the directional charge transport in thin films, I used the TRM-SHG method that can image vectorial pathways of carrier motion within the film of organic semiconductors[69-71]. Although I-V curve tracing and TOF measurements are very useful in terms of giving information on carrier transport anisotropy, they failed to specify the exact directions of the highest and the lowest carrier mobility for their inherent limited angular a panoramic view of carrier mobility, which enables the determination of the directions of both superior and inferior mobility along with their magnitude from the image itself[72]. Furthermore, TRM-SHG probes directly into the heart of the transport phenomenon, giving an instantaneous judgment of the inherent anisotropy of mobility along with the related activation energies[30]. The technique EFISHG was utilized to explore carrier distribution in thin film devices. If a static electric field  $E(0)$  is applied and the material is concurrently irradiated with a powerful laser beam, then there is a second-

order nonlinear polarization response that is elicited [33]. The response is described in the following *equation 2.1*.

$$\mathbf{P}_{(2\omega)} = \epsilon_0 \chi^{(2)} \mathbf{E}(\omega) \mathbf{E}(\omega) + \epsilon_0 \chi^{(3)} \mathbf{E}(0) \mathbf{E}(\omega) \mathbf{E}(\omega) \quad (2.1)$$

In this equation the first term represents the standard SHG effect. It is natural that in the symmetrical material this term has a zero value; for there is no natural SHG in a material under symmetrical conditions. The second term is caused by the action of the static electric field  $E(0)$ . It is the source of the SHG signal in symmetrical materials if an electric field is applied. The basis of this interaction forms the EFISHG effect, in which the static electric field  $E(0)$  is composed not only of an externally imposed field  $E_{\text{ext}}$  but also includes the intrinsic space-charge field  $E_{\text{sc}}$ [34]. Monitoring the EFISHG signal provides a very detailed mapping of carrier distribution and enlightens the spatial properties of carrier dynamics.

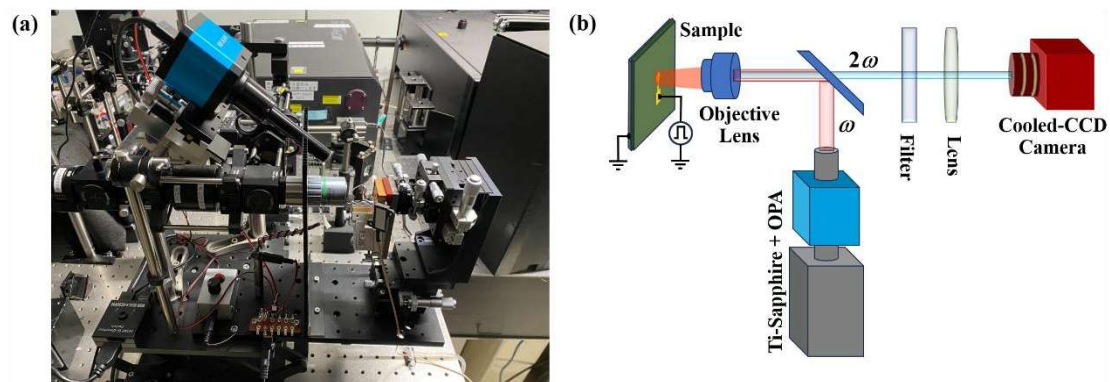


**Figure 2.17** (a) Setup of TRM-SHG (b) Schematic representation of the TRM-SHFG setup.

This technique, now spread into a time-resolved format, opens up opportunities for live tracking of transient phenomena in carrier distribution. The device schematic and image is provided in **Figure 2.17**. The TRM-SHG is an advanced device that plots real-time pictures of carrier action through manipulation of the delay time[71]. It is the delay time that is

referred to as the time lapse between the induction of a voltage pulse to the device and the onset of the laser pulse. This method allows giving a holistic view of the activities of carriers inside the device while integrating spatial distribution and temporal evolution to provide a full view of internal processes controlling carrier dynamics.